Steady State and Transient Analysis of Heat Conduction in Nuclear Fuel Elements

ROZHGAR OTHMAN

KTH Numerical Analysis
and Computer Science

Master's Degree Project
Stockholm, Sweden 2004

TRITA-NA-E04051

Numerisk analys och datalogi
KTH
100 44 Stockholm

Department of Numerical Analysis
and Computer Science
Royal Institute of Technology
SE-100 44 Stockholm, Sweden

Steady State and Transient Analysis of Heat Conduction in Nuclear Fuel Elements

ROZHGAR OTHMAN

TRITA-NA-E04051

Master's Thesis in Numerical Analysis (20 credits)
at the Scientific Computing International Master Program,
Royal Institute of Technology year 2004
Supervisor at Nada was Gerd Eriksson
Examiner was Axel Ruhe

Steady State and Transient Analysis of Heat Conduction in Nuclear Fuel Elements.

Abstract

A radial heat conduction model for fuel elements in fuel, cladding and gap has been developed. It takes the temperature and burn-up dependence of thermo physical data of UO2 and Zircaloy-2 into account, thus improving the fidelity over the current version of the core stability prediction tool MATSTAB2. The thermo physical data has been implemented in a MATLAB library of material property functions.

The non-linearity requires a new numerical method, and a second order finite difference scheme has been developed. The new model runs in steady state or transient mode with the standard MATLAB time integrator ODE15S. A first version has been adapted to run with MATSTAB2. The run-time is about fifty minutes for a case with 8500 radial slices and 10 nodes per slice. However, the code can be easily optimised to run at least a factor five faster without changing the computed results.

Stationär och transient analys av värmeledning i kärnbränsleelement .

Sammanfattning

En radiell värmeledningsmodell har utvecklats för bränsleelement bestående av kärnbränsle, luftgap och kapsling. Den tar hänsyn till hur de termofysikaliska parametrarna för urandioxid och zircaloy-2 beror av temperaturen och, för urandioxidens del, av graden av utbrändhet. Därmed utgör modellen en förbättring av det nuvarande beräkningsverktyget MATSTAB2.

Temperaturberoendena modelleras med ickelinjära funktioner och har implementerats i ett MATLAB-bibliotek. Ickelineariteten kräver en ny numerisk metod och vi har utvecklat ett finitadifferensschema och implementerat det i MATLAB. Detta ger den stationära lösningen och för den transienta används MATLABs inbyggda ODE15S-integrator. En preliminär version har provkörts ihop med MATSTAB2. För ett fall med 8500 cirkulära skivor och 10 noder per skiva blev körtiden hela femtio minuter. Några enkla optimeringar torde kunna sänka tiden till en femtedel eller mindre utan ändring i beräkningsresultaten.

Contents

Table Of Figures

1. Introduction

Many computer codes used by Vattenfall Fuel for e.g. transient and stability analysis of Boiling Water Reactors (BWR) require a heat conduction model for the nuclear fuel elements.

Predicting the core stability characteristics requires the simulation of the thermal-hydraulics and the neutronics as well as their mutual interactions. The usual approach is to consider the stability of small perturbations by a linearized model around a steady state. The linearized model is very large, $O(10^5)$ states, and special eigenvalue calculation methods have been developed for the problem. MATSTAB2 [2] is a new stability prediction code built in MATLAB, which uses these techniques. The physical model implemented in MATSTAB2 was taken from the BWR core simulator RAMONA-3B [1] that solves the coupled partial differential equations of water-steam two-phase flow and neutronics by time stepping. The MATSTAB2 model has been simplified and does not contain all the features and details implemented in RAMONA.

1.1. Project Objectives

The project investigates the development of a higher-fidelity thermal fuel element model. The new model takes into account the variation of thermophysical data; such as thermal conductivity and heat transfer coefficients, with temperature and burn-up. The model is a radial conduction model for a slice of a fuel rod and is to be used for transient as well as steady state calculations. A pilot version of the model is tested in the MATSTAB2 environment to assess run-times, memory requirements, etc., with an eye to later implementation of an optimized model.

1.1.1. Burn-up and Temperature Dependent Thermophysical Data

The radial fuel element model is coupled to the existing transient two-phase flow model of the cooling fluid channel and calculates the fuel pin surface heat flux and temperature distribution including the effects of the cladding and the fuel/cladding gap. The boundary conditions at the cooling fluid interface are time dependent and can be specified in terms of flow conditions. Development of advanced model of heat conduction that allows specification of thermophysical properties dependent on two parameters, by interpolation in tables, or as closed functional forms is the first task.

1.1.2. New Numerical Method for Radial Heat Conduction

The existing MATSTAB model assumes constant transport coefficients. To achieve the accuracy improvement provided by the new material property functions, a new numerical method was developed. It uses a standard second order accurate finite difference scheme with a graded mesh. The transient model uses the standard MATLAB integrator ODE15S.

The steady state model uses the Newton scheme for solution of the non-linear system. The Jacobian is computed by finite differences.

1.1.3. Tests in the MATSTAB2 environment

A first version of the code has been adapted to run in MATSTAB [2]. Initial timing results indicate that the run-time can be reduced by a factor of (at least) five by changing the Jacobian finite differencing to take the tri-diagonal pattern into account, by pre-computing and storing a number of quantities, and by optimizing arithmetic expressions. These changes do not change the computed results.

2. Background

2.1. Power Reactors

There are several types of power reactors. Two distinct light-water cooled nuclear reactor steam supply systems are commercially available: the *Boiling Water Reactor* (BWR) system and the *Pressurized Water Reactor* (PWR) system. The BWR steam supply system is attractive due to its basic simplicity and potential for greater thermal efficiency, better reliability, and lower capital cost than other competing light water reactor systems.

2.1.1. Technical Description of BWR

The reactor tank contains the reactor fuel, uranium, in the form of fuel rods collected into fuel elements. The BWR core is comprised essentially of three components: fuel assemblies, control rods, and in-core neutron flux monitors. The fuel is cooled by water pumped up by the main circulation pump through the reactor core containing the fuel. The water reaches boiling point in the reactor core and the water-steam mixture separates into water and steam, the dry steam is led to the turbine plant, which drives the electricity generator. The steam is condensed in the condenser, which is cooled by e.g. sea water. The reactor output is controlled by means of control rods inserted through the bottom of the reactor tank.

2.1.1.1. Fuel Assembly

The core consists of fuel assemblies in square arrays. A number of fuel rods and water rods, so designed that water flowing through them provides additional moderation, are contained in each assembly. Each fuel assembly is contained in a four -sided channel box , which prevents cross flow of coolant between assemblies. A control rod with cruciform cross section is located within each set of four assemblies.

Fuel Pellets

The fuel elements are composed of a stack of cylindrical Uranium oxide UO2 fuel pellets. These pellets are enclosed in hollow Zircaloy-2 tubes, which serve to contain the radioactive fission products and to protect the UO2 pellets from the steam-water environment in the rod bundles. The thermal properties and physical characteristics of UO2 and Zircaloy are discussed in Chapter (3.) Of particular interest is the temperature dependence of UO2 thermal conductivity. The effect of burnup on UO2 thermal conductivity, which is ignored in RAMONA-3B [1] heat conduction model, is considered in section (3.1.1.).

Zircaloy-2 Enclosure

The Zircaloy-2 cladding material is a well-known reactor material. It is chosen for using in BWR fuel elements because it has superior properties of strength, corrosion resistance, and neutron economy. This means Zircaloy-2 has a relatively small neutron capture cross section. In sections (3.3.1)-(3.3.3) temperature-dependent Zircaloy-2 properties, thermal conductivity, heat capacity and density have been investigated and calculated.

Fuel Pellet –Zircaloy Tube Gap

On initial loading of the fuel pellets, there is a small diametric gap between the surface of the fuel pellets and the inside surface of the Zircaloy-2 cladding. Before initial operation, this gap is filled with helium gas. Helium has a relatively high thermal conductivity so that the operating temperature drop across the gap is minimized. Subsequent to initial operation, small quantities of fission gases such as xenon and krypton are released. These gases have fairly low thermal conductivity compared to the helium hence in the absence of any other effects we might expect that the gap temperature difference (ΔT) would increase with irradiation. However shortly after initial operation the gap essentially is closed. This gap closure occurs due to:

- Thermal stress-induced cracking and relocation of the UO2 pellets.
- The fact the fuel pellets are at a higher temperature than the cladding and have a coefficient of thermal expansion about twice that of the Zircaloy-2 cladding.

The main problem of fuel rod behaviour modelling is the determination of the heat transfer coefficients h_{gap} at the gas gap between fuel and cladding and h_{wall} from the cladding surface to the coolant h_{gap}, has been found from table-2 [9], however two models have been introduced for finding it, the first model equation (3-12) depending on the fresh gas thermal conductivity and the geometrical gap width, and the second model equation (3-13) depending on the heat transfer coefficients for conduction between the layers, fuel, gap and cladding, section (3.2).The process of convective heat transfer is a very important mechanism for the transport of energy from nuclear reactor fuel rods. Section (3.4.1.) is concerned with single-phase convective heat transfer mode.

Now that the fuel element geometry, thermal properties and physical characteristics have been described we can consider the thermal analysis of typical BWR fuel elements by solving the classical heat conduction model equation (4-1) as it is described and calculated in Chapter-4 and 5.

2.1.1.2. Nuclear-Coupled Thermal Hydraulic Flow

An important BWR consideration is the reactor stability depending on the coupled hydrodynamic-neutronic feedback response resulting from the formation of steam in the core.

Each transient of the reactor involves two feedback effects:

- The thermal-hydraulic effect
- The neutron kinetics effect

The thermal-hydraulic feedback is strongly affected by the *density-wave* mechanism, and it is a function of the channel boundary condition. It involves physical mechanisms that cause density-wave oscillations in a single flow channel. Usually, the power generated is assumed constant throughout a density wave transient. The second mechanism, the neutron kinetics feedback, involves the temperature and heat flux in the fuel directly and is of immediate interest here.

As described above the power generation in the fuel is assumed to be constant in the thermal hydraulic feedback. However, in a BWR flow channel, the power generation in the fuel is in general not constant. It depends on the neutron kinetics, which determines the power generated in the fuel, and hence determines the temperature distribution in the fuel rod and accordingly the heat flux from the fuel to the coolant.

2.1.1.3. Neutron Kinetics Feedback

There are two main neutron-kinetics (reactivity) feedback mechanisms in a BWR:

- The void reactivity feedback
- Doppler feedback

The power generation in a BWR is strongly affected by the void reactivity feedback mechanism, whereas the Doppler feedback –which is related to the temperature in the fuel rod, is weaker. The fuel rod (heat conduction) dynamics is affected directly by the power changes, which introduce fuel rod temperature changes and additional time-delay between changes in the power level and the resulting changes in the heat flux from the surface of the fuel rod to the surrounding coolant in the flow channel. Thus the fuel rod dynamics determines the time scale on which the neutron kinetics feedback affects the thermal-hydraulics. Finally, the Doppler feedback, of course, depends directly on the fuel rod temperature, and any change in the fuel rod temperature results in a change via this feedback mechanism.

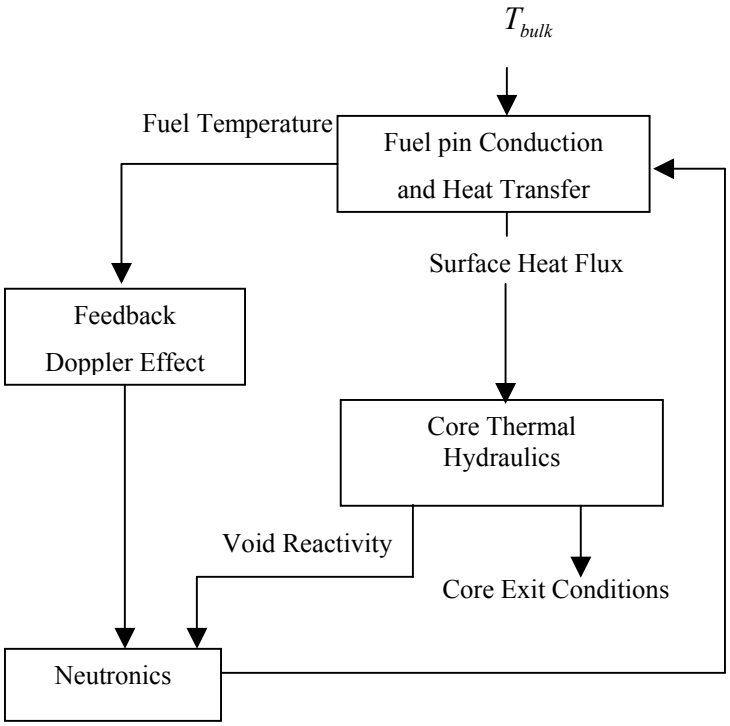

Figure 2-1: Neutronic/ Thermal Hydraulic Feedback System in a BWR [2]

2.1.1.4. Temperature effects on reactivity

Changes in the fuel temperature, which results from a change of power, can cause change in reactivity, which in turn affect the power. Thus a feedback process in established with an important bearing on the safety of the reactor. For instance, if an increase in power followed by an increase in the temperature of parts of a reactor causes an increase in reactivity, this will lead to further increase in power and an unstable situation will exist which, if it is not controlled, could lead to an accident. On the other hand, if an increase in power and temperature leads to a decrease in reactivity, the original power rise will be retarded and a stable situation will exist in which the reactor tends to control itself.

When a reactor undergoes a power increase, the resulting temperature changes in different components of the reactor occur at different rates. The fuel temperature will rise at nearly the same rate as the power with little or no lag. The coolant temperature will rise more slowly because of the time lag in the transfer of heat form the fuel to the coolant.

2.1.1.5. Modelling of Fuel Rod Heat Conduction

A fuel rod consists of UO2 pellets in a Zircaloy-2 cladding tube and a small gap between the surface of the fuel pellets and the inside surface of the cladding, the figure below.

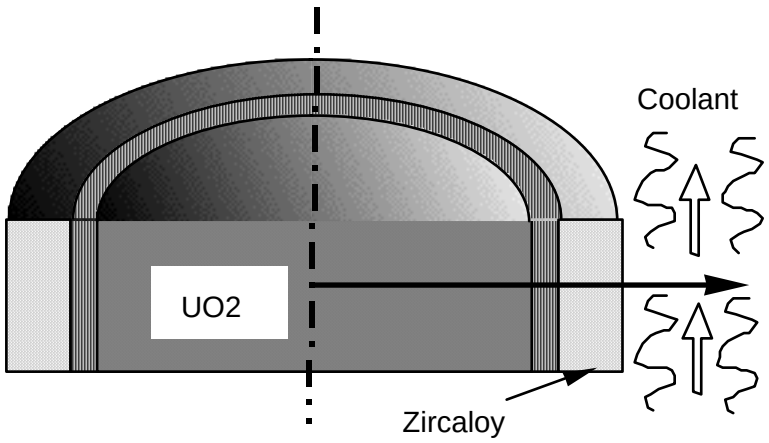

The heat generated by nuclear fission is conducted through the fuel rod and convected by the surrounding coolant in the flow channel. A radial heat conduction model is used to calculate the fuel heat flux and temperature distribution.

The thermal energy storage and transport is modelled with the following assumptions:

- Axial and azimuthal conduction is negligible.
- Volumetric heat generation q''' is uniformly distributed over the fuel pellet cross-section, gamma heat generation in the gas gap and the cladding is ignored.
- Thermal conductivity in the fuel pellet and the cladding depends on temperature, burn up and porosity.
- Volumetric heat capacity and density in fuel pellet and cladding are temperature dependent.
- Thermal conductance in the gas gap is a function of temperature and burn up.

3. Thermo-physical Properties

3.1. Thermal Properties of UO2

Uranium dioxide (UO2) is a standard fuel of modern nuclear power plants. The main advantages in the use of uranium dioxide are its high melting point, dimensional and radiation stability and its chemical compatibility with other reactor components. The main disadvantages are its low thermal conductivity and low fuel density, which leads to high centreline temperatures and large volume cores. The relatively low thermal conductivity of UO2 requires that large temperature gradients are established to drive the heat from the fuel.

3.1.1. Thermal Conductivity

The material property having one of the largest effects on reactor fuel behaviour is thermal conductivity. Poor thermal conductivity will result in a large difference between the fuel centreline and surface temperature in order to remove the fission heat. This may cause the fuel centreline temperature to operate close to its melting point and limit available power.

The recommended correlation for the thermal conductivity of solid UO2 is from INSC [8]. This equation was selected because it is the best equation available from a theoretical aspect; it is in good agreement with other equations that are based on statistical fits to the experimental data.

In crystalline solids such as the UO2 fuel there are three major heat transport mechanisms. At temperatures < 2000K, heat transfer is dominated by lattice vibrations. Above 2000K radiation and electron contributions become important.

Porosity and burn up affect thermal conductivity. Fuel burn up reflects the effects of fission products dissolved in the metal matrix, precipitated fission products, fission product gas bubbles, and radiation damage.

$$k_f = ko \cdot fd \cdot fp \cdot fr \cdot fm \tag{3-1}$$

where:

$$ko = \frac{1}{0.0375 + 2.165 \cdot 10^{-4} T} + \left(\frac{4.715.10^{9}}{T^{2}}\right) \cdot e^{\frac{-16361}{T}} \tag{3-2}$$

fd is the effect of the dissolved fission products,

We define $bval = \frac{b}{9.383}$ then,

$$fd = \left[\frac{1.09}{bval^{3.265}} + \frac{0.0643}{\sqrt{bval}}\sqrt{T}\right] \cdot \arctan\left[\frac{1.09}{bval^{3.265}} + \frac{0.0643}{\sqrt{bval}}\sqrt{T}\right] \tag{3-3}$$

fp is the effect of the ‘’precipitated’’ fission products ,

$$fp = 1 + \frac{0.019.bval}{3 - 0.019.bval}\left[\frac{1}{1 + e^{(1200-T)/\ 100}}\right] \tag{3-4}$$

fr is the effect of the radiation,

$$fr = 1 - \frac{0.2}{1 + e^{(T-900)/80}} \tag{3-5}$$

Fuel porosity reduces thermal conductivity and gross swelling, we can find porosity by knowing the volume of the pores and volume of the solid, or we can find it by taking the difference of the fully dense density of UO2 and theoretical density:

$$p = \frac{\left(\rho_{td} - \rho\right)}{\rho_{td}}$$

ρ_{td} is theoretical density of UO2

ρ is fully dense density of UO2

The effect of porosity is accounted for by the Maxwell-Eucken factor, fm,

$$fm = \frac{1 - p}{1 + (s-1)p} \tag{3-6}$$

T is temperature (K)

b is burn up in atom% (1 atom% = 9.383GWD/MTU at 200MeV/fission)

s is shape factor of the pores

The thermal conductivity of solid UO2 as a function of temperature and burn up is shown in figure (3-1).

3.1.2. Heat capacity

Accurate knowledge of the specific heat of the fuel material is needed for assessment of reactor behaviour under transient conditions. According to the equations recommended by INSC [8]:

$$C_P = \left[\frac{b_1 b_4{}^2 e^{\Theta}}{T^2\left[e^{\Theta} - 1\right]^2} + 2b_2 T + \frac{b_3 b_5}{b_6 T^2} e^{\frac{-b_5}{b_6 T}}\right] \tag{3-7}$$

where $\Theta = \frac{b_4}{T}$

C_P is specific heat capacity $J/kg.K$

T is fuel temperature K

$b_1 = 19.145\, J/kg \cdot K$ $\quad b_2 = 7.8473.10^{-4}\, J/kg.K^2$

$b_3 = 5.6437.10^6\, J/kg$ $\quad b_4 = 535.285K$

$b_5 = 37695$ $\quad b_6 = 1.987$

The heat capacity of U02 as a function of temperature is shown in figure (3-2).

3.1.3. Density

We can find the density of UO2 by assuming that:

$$\rho = F_{td} \cdot \rho_{UO2} \tag{3-8}$$

ρ_{UO2} is theoretical density of fully dense UO2 ($= 1.097 \cdot 10^4\ kg/m^3$)

F_{td} is fractional of theoretical density (=0.95)

ρ is UO2 density (kg/m^3)

In this report the recommended equations for the density of solid Uranium dioxide are taken from INSC [2] properties. The density as a function of temperature is calculated from:

$$\rho(T) = \rho(273)\left(\frac{L(273)}{L(T)}\right)^3 \tag{3-9}$$

where:

ρ (273) is the density of UO2 at 273K($= 10.956\ Mg/m^{-3}$),
L (273) and L (T) are the lengths of solid Uranium at 273K and at temperature T (K), respectively.

The ratio of the length at 273K to the length at temperature T (K) may be calculated from INSC [8] equations for the thermal expansion of solid U02:

- For 273K≤T≤923K

$$L(T) = L(273)(A_1 + B_1T - C_1T^2 + D_1T^3) \tag{3-10}$$

$A_1 = 9.9734 \cdot 10^{-1}$ $\quad B_1 = 9.802 \cdot 10^{-6}$

$C_1 = 2.705 \cdot 10^{-10}$ $\quad D_1 = 4.291 \cdot 10^{-13}$

- For 923K≤T≤3120K

$$L(T) = L(273)(A_2 + B_2T - C_2T^2 + D_2T^3) \tag{3-11}$$

$A_2 = 9.9672 \cdot 10^{-1} \quad B_2 = 1.179 \cdot 10^{-5}$

$C_2 = 2.429 \cdot 10^{-9} \quad D_2 = 1.219 \cdot 10^{-12}$

The density as a function of temperature of solid U02 is shown in figure (3-3).

3.2. Fuel/Cladding Gap Heat Transfer

The gap between the fuel and cladding contains a mixture of fuel rod filled gases, more often Helium (because of its high thermal conductivity) and gaseous fission products that have been released form the fuel. The gas gap heat transfer coefficients h_{gap} for fresh fuel gas can be expressed as:

$$h_{gap} = \frac{k_{gas}}{\delta_{eff}} \tag{3-12}$$

where,

k_{gas} is thermal conductivity of the gas

δ_{eff} is the effective gap width

Or as:

$$h_{gap} = h_s + h_f + h_r \tag{3-13}$$

where:

h_{gap} total gap conductance

h_s heat transfer coefficients for conduction through fuel/cladding contact spots

h_f heat transfer coefficients for conduction through the gas layer at the fuel/cladding interface

h_r radiant heat transfer coefficient

The equation (3-13) is used to describe the heat gap conductance for all design calculations of BWR fuel rods. Figure (3-7), solid lines, shows h_{gap} as a polynomial function, second degree in temperature and third degree in burn up.

The symbols are the data points to which the polynomials were fitted, see [9].

3.3. Cladding : Zircaloy-2

The cladding prevents the escape of fission products to the coolant. Zirconium alloys have been used in a number of water–cooled fission reactor types due to their excellent aqueous corrosion resistance, low thermal neutron absorption cross section and good mechanical properties. The most popular is Zircaloy-2.

3.3.1. Thermal conductivity

The recommended equation from INSC [8] for the thermal conductivity of Zircaloy-2 is:

$$k_c = a_o + a_1 \cdot T + a_2 \cdot T^2 + a_3 \cdot T^3 \qquad (3\text{-}14)$$

a_o =7.51 a_1 =$2.09 \cdot 10^{-2}$

a_2 =$-1.45 \cdot 10^{-5}$ a_3 =$7.67 \cdot 10^{-9}$

k_c thermal conductivity of cladding, $W / m.K$

T cladding temperature, K

The thermal conductivity as a function of temperature of Zircaloy-2 is shown in figure (3-4).

3.3.2. Heat Capacity

The recommended equation from INSC [8] for the heat capacity of Zircaloy-2 in the α phase is:

for 273<T<1100K:

$$c_p = 255.66 + 0.1024T \qquad (3\text{-}15)$$

In the β- phase the behavior is quadratic:

for 1320K<T<2000K

$$c_p = 597.1 - 0.4088T + 1.565 \cdot 10^{-4} T^2 \qquad (3\text{-}16)$$

Zircaloy-2 heat capacity data in the (α+β)- phase is:

for 1100<T<1214

$$c_p = Eq\ (3\text{-}15) + 1058.4\, e^{\frac{(T-1213.8)^2}{719.61}}$$

for 1214<T<1320

$$c_p = Eq\ (3\text{-}16) + 1058.4\, e^{\frac{(T-1213.8)^2}{719.61}} \qquad (3\text{-}17)$$

Where temperatures are in K and heat capacity in $J / kg.K$.

Cladding specific heat as a function of temperature is shown in figure (3-5).

3.3.3. Density

The Zircaloy-2 density as a function of temperature has been calculated from the room temperature density, $6501 kg/m^3$, and the change in volume obtained from the linear thermal expansion. The density for the α-phase (T<1083K) is calculated by the linear equation:

$$\rho = 6690 - 0.1855 \cdot T \qquad (3\text{-}18)$$

Where ρ is the density in kg/m^3 and T is the temperature in K.

The density as a function of temperature of Zircaloy-2 is shown in figure (3-6).

3.4. Coolant

The coolant, which passes through the nuclear reactors, is used to transport the reactor heat either to a boiler where steam is raised to run a conventional turbine or it is used as a thermodynamic heat engine fluid and passes directly into the turbine and back to the reactor. Boiling water and some gas cool reactors use the coolant directly in the turbine. Some desirable properties for a coolant include:

- High heat transport and transfer coefficient (so as to pick up the maximum amount of heat and moves elsewhere).
- Low melting point.
- Low neutron absorption cross section.
- Radiation and thermal stability.
- Low viscosity (in order not too much power needed to pump it).

The coolants in common use include:

- Light or heavy water
- Liquid metal
- Liquid organics
- Air, helium, or carbon dioxide gases

Water is used in most commercial reactors today; in this case, the water is dual purpose since it also serves a moderator (i.e. it slows the neutrons down to thermal energy to increase the likelihood of fission. Heat transfer form the clad surface to the coolant is described by a heat transfer coefficient,

$$q_{wall} = h_{wall}(T_b - T_c)$$

Where h_{wall} is convective heat-transfer coefficient, T_b is bulk temperature and T_c is outer clad surface temperature.

This coefficient depends upon the properties and flow conditions of the coolant.

3.4.1. Forced Convection Heat Transfer

We consider the dominant mode of convective heat transfer to be single-phase convection. The convective heat transfer coefficient h_{wall} is usually expressed in

terms of the thermal conductivity of the fluid k, the hydraulic diameter of the channel D_h and a dimensionless parameter Nu.

For single phase forced convection, the Dittus–Bolter correlation s given by,

$$h_{wall} = (k / D_h) Nu \tag{3-19}$$

where Nu is known as the Nusselt number which characterizes both the physical properties of the fluid and the dynamical characteristics of its flow.

$$Nu = 0.023 \,\mathrm{Pr}^{0.4}\, \mathrm{Re}^{0.8} \tag{3-20}$$

$$\mathrm{Re} = \rho u_z D_h / \mu \tag{3-21}$$

$$\mathrm{Pr} = \frac{\Delta}{=} \frac{C_p \mu}{k} \tag{3-22}$$

Re is the Reynolds number

Pr is the Prandtl number

where μ, c_p are the dynamic viscosity and specific heat of the fluid.

We can define D_h by

$$D_h = 4S / Z \tag{3-23}$$

where S is the flow area and Z is the wetted perimeter of the flow. As an example, consider a bundle of circular fuel elements of diameter *d* and square pitch *p*. Then the equivalent hydraulic diameter can be defined by locating a unit cell and calculating *S* and *Z* for this cell as:

$$S = p^2 - \pi d^2 / 4$$
$$Z = \pi d$$

The hydraulic diameter for triangular lattice geometries can be obtained in a similar way,

$$D_h = d\left[\frac{4}{\pi}\left(\frac{p}{d}\right)^2 - 1\right] \tag{3-24}$$

Finally one can get,

$$h_{wall} = 0.023\left(\frac{k}{D_h}\right).\left(\frac{\rho u D_h}{\mu}\right)^{0.8}.\left(\frac{C_p \mu}{k}\right)^{0.4} \tag{3-25}$$

If the bulk temperature of the fluid is known then it can be used to determine the thermodynamic properties and by using Eq (3-25) we can calculate convective heat transfer coefficients h_{wall}. But in our calculations we have h_{wall} as a given data.

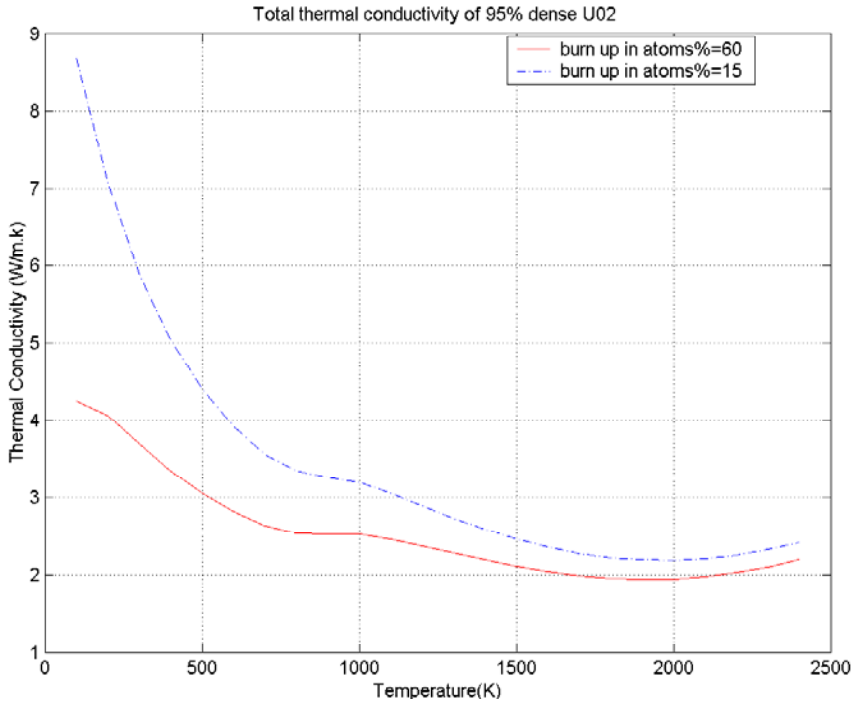

Figure 3-1

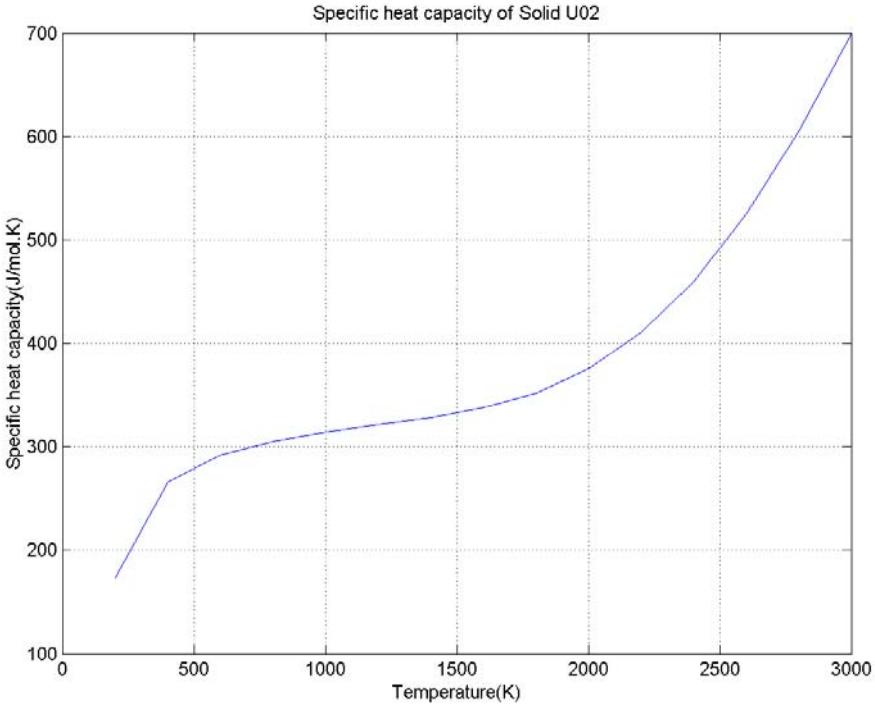

Figure 3-2

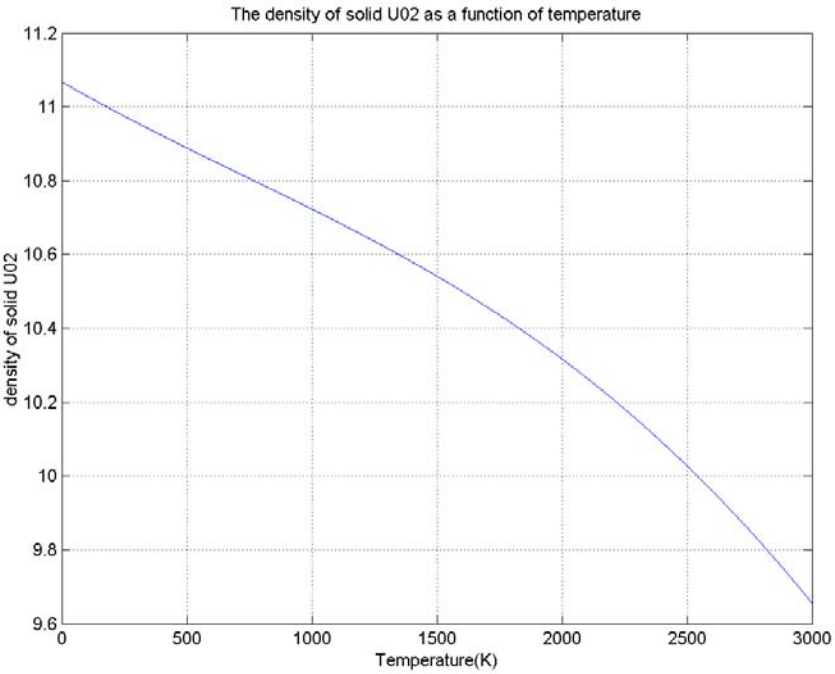

Figure 3-3

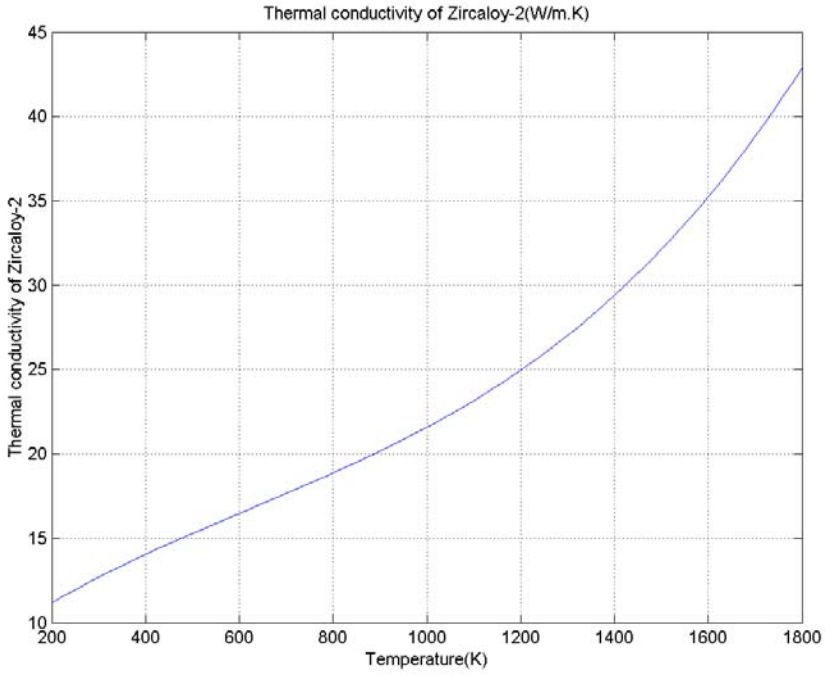

Figure 3-4

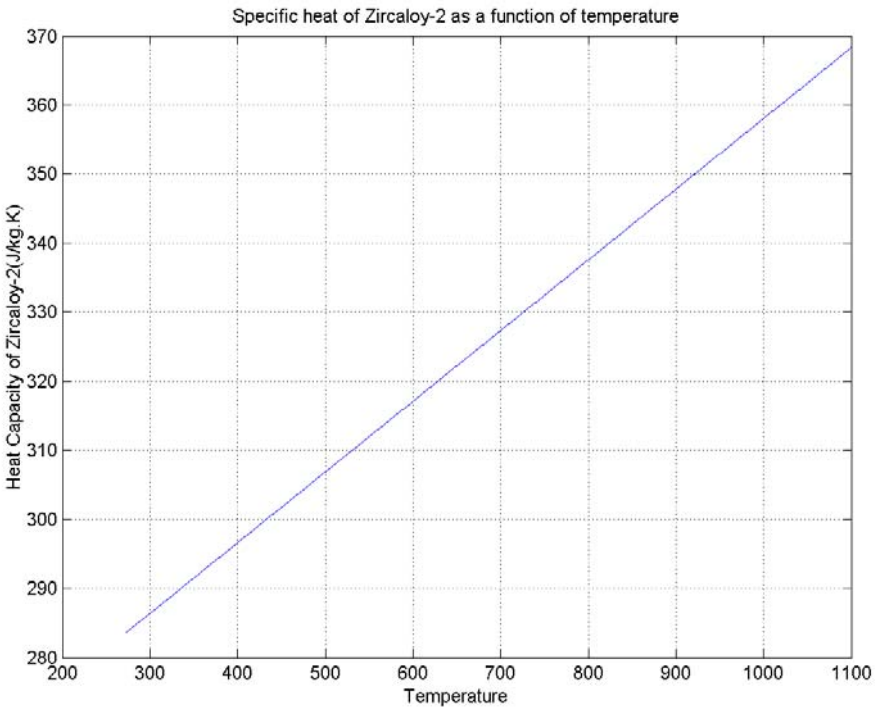

Figure 3-5

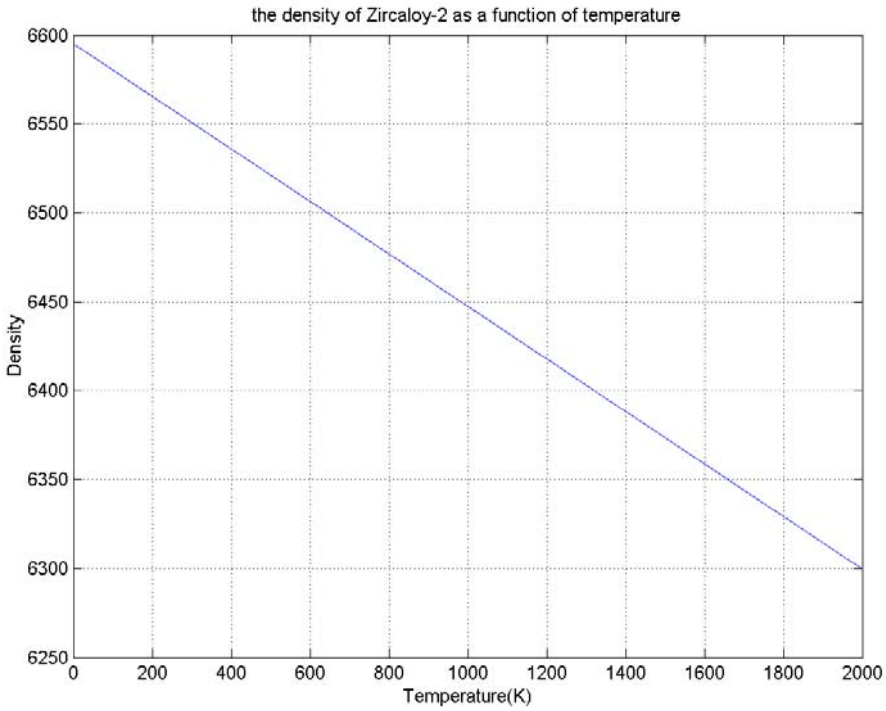

Figure 3-6

Gap Heat Transfer Coefficients as a

Function of Temperature and Burn up

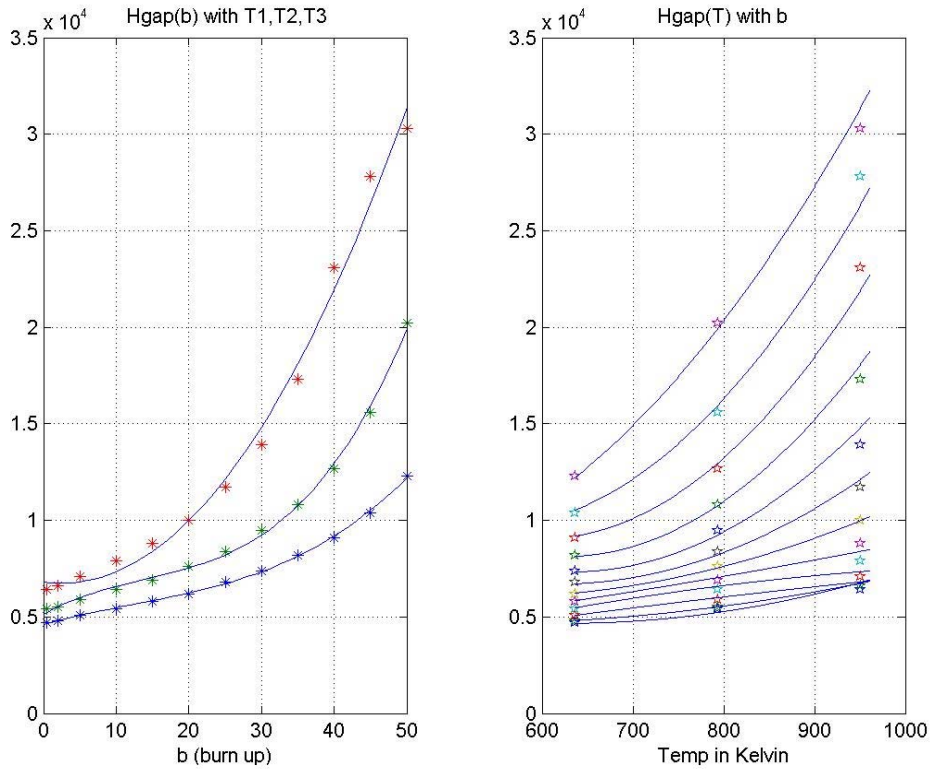

Figure 3-7

4. Radial Heat Conduction in Nuclear Fuel Elements

Power reactor cores are composed of cylindrical fuel elements that contain fuel pellets, gap and cladding. Our goal will be to calculate the temperature drop from the centre line of the fuel where the maximum temperature occurs to the surface of the clad in terms of the various physical properties of the fuel elements, while the fuel element geometry, thermal properties, and physical characteristics have been known. Further we consider the thermal analysis of a BWR fuel element. This analysis yields the transient and steady state temperature distributions required in the design/ safeguards analysis of a BWR. The general procedure is to solve the classical heat conduction equation

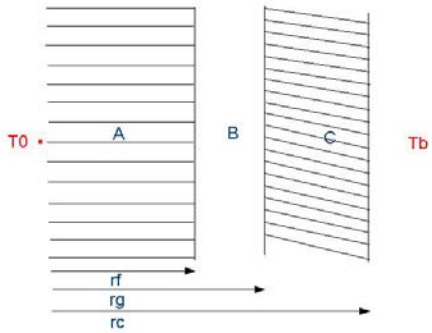

$$\frac{1}{r}\frac{\partial}{\partial r}\left(kr\frac{\partial T}{\partial r}\right)+q'''=\rho Cp\frac{\partial T}{\partial t} \tag{4-1}$$

And the boundary conditions are given by:

$$-k_c\frac{\partial T}{\partial r}\bigg|_{r=rc}=q''(r_c,t)=h_{wall}\left(T_c(t)-T_b(t)\right) \tag{4-2}$$

$$-k_f\frac{\partial T}{\partial r}\bigg|_{r=rf}=q''(r_f,t)=\left(\frac{r_g}{r_f}\right)q''(r_g,t) \tag{4-3}$$

$$-k_c\frac{\partial T}{\partial r}\bigg|_{r=rg}=q''(r_g,t)=h_{gap}\left(T_f(t)-T_g(t)\right) \tag{4-4}$$

For all the notations we refer to Appendix A.

We will use two techniques to solve this equation. One technique is to write this parabolic partial differential equation in finite difference form and to solve it numerically with the appropriate initial and boundary conditions.

Another approach is to attempt to obtain an exact analytical solution. That is a quite complex process for the transient case, involving Bessel functions of various types and orders. Additionally, the non-linearities must be neglected, so the analytical transient solutions are of limited value and will not be pursued further here. However, the steady solutions are easy and give rough-and-ready answers.

4.1. Analytical Solution of Steady-State Heat Conduction

4.1.1. Fuel

The heat conduction equation for a cylindrical fuel pin with a uniform volumetric heat source q''' in which axial heat conduction can be ignored takes the form,

$$\frac{1}{r}\frac{d}{dr}\left(k_f\, r\frac{dT}{dr}\right)=-q''' \tag{4-5}$$

$$\frac{d}{dr}\left(k_f\, r\frac{dT}{dr}\right)=-q'''\, r \tag{4-6}$$

$$d\left(k_f\, r\frac{dT}{dr}\right)=-q'''\, r\, dr \tag{4-7}$$

Assuming that k is constant, then by integrating, equation (4-7) becomes,

$$k_f r\frac{dT}{dr}=-\frac{r^2}{2}q'''+C_1 \tag{4-8}$$

$$\left.\frac{\partial T}{\partial r}\right|_{r=0}=0 \tag{4-9}$$

Then,

$$C_1=\frac{r^2}{2}q'''\big|_{r=0} \quad \Rightarrow C_1=0$$

by integrating equation (4-8) we get,

$$k_f\frac{dT}{dr}=-\frac{r}{2}q''' \tag{4-10}$$

$$k_f T=-\frac{r^2}{4}q'''+C_2 \tag{4-11}$$

For r=0, the temperature is T_0 and $C_2=k_f T_0$ so,

$$T=T_0-\frac{r^2}{4k_f}q''' \tag{4-12}$$

and for $r = r_f$ we have,

$$T_0 - T_f = \frac{r_f^{\,2}}{4k_f} q''' \tag{4-13}$$

Introducing the linear power density of the fuel element as:

$$q' \equiv \pi r_f^{\,2} q''' \tag{4-14}$$

then equation (4-12) can be written in terms of q''' as

$$\Delta T\big|_{Fuel} = T_0 - T_f = \frac{q'}{4\pi k_f} \tag{4-15}$$

4.1.2. Gap

Since there is no heat generation in the gap, we would solve

$$\frac{1}{r}\frac{d}{dr}\left(k_g\, r \frac{dT}{dr}\right) = 0 \tag{4-16}$$

We assume that k_g = constant, by integrating, equation (4-16) becomes,

$$k_g r \frac{dT}{dr} = C_1 \tag{4-17}$$

Heat flux at the fuel surface, $q'' = \frac{q'}{2\pi r_f}$, $q' = \pi r_f^{\,2} q'''$

Where q' is the linear power density of the fuel element.

$\therefore \quad q'' = \frac{q''' r_f}{2}$

According to continuity of heat flux at the fuel surface,

$$q'' = -k_g \left.\frac{dT}{dr}\right|_{r=r_f} = \frac{q''' r_f}{2}$$

But from Eq (4-17), $k_g r \frac{dT}{dr} = C_1$ then,

$$C_1 = -\frac{q''' r_f^2}{2} \tag{4-18}$$

$$k_g r \frac{dT}{dr} = -\frac{q''' r_f^2}{2} \tag{4-19}$$

$$\int_{T_f}^{T_g} dT = \int_{r_f}^{r_g} \frac{dr}{r} \frac{q''' r_f^2}{2k_g} \tag{4-20}$$

$$\Delta T\big|_{gap} = T_g - T_f = -\frac{q''' r_f^2}{2k_g} \ln\left(\frac{r_g}{r_f}\right) \tag{4-21}$$

$$r_g = r_f + t_g \tag{4-22}$$

Since t_g (gap thickness) is usually very small, we can expand the log term to write

$$\Delta T\big|_{gap} = -\frac{q''' r_f}{2} \frac{t_g}{k_g} = \frac{q'}{2\pi r_f}\left(\frac{t_g}{k_g}\right) \tag{4-23}$$

After a period of operation the gap will contain a mixture of the original gas and fission product gases, hence the thermal conductivity k_g will change over core life. We define an effective coefficient of gap heat transfer h_{gap} such that the temperature drop across the gap is:

$$\Delta T\big|_{gap} = -\frac{q''}{h_{gap}} \tag{4-24}$$

The heat flux across the gap in steady state must be just the amount of heat produced in the fuel divided by the surface area of the fuel:

$$q'' = -\frac{q'''\left(\pi r_f^2 \Delta T\right)}{2\pi r_f \Delta T} = \frac{q''' r_f}{2} = \frac{q'}{2\pi r_f} \tag{4-25}$$

$$\Delta T\big|_{gap} = \frac{q'}{2\pi r_f h_{gap}} \tag{4-26}$$

Here we have h_{gap} instead of k_g, and the range of temperature difference depends on the value for h_{gap}.

4.1.3. Cladding

Since there is no heat generation in the cladding, we would solve

$$\frac{1}{r}\frac{d}{dr}\left(k_c\, r\frac{dT}{dr}\right)=0 \tag{4-27}$$

$$k_c r\frac{dT}{dr}=C_1 \tag{4-28}$$

According to continuity of heat flux at the fuel surface,

$$-k_c\left.\frac{dT}{dr}\right|_{r=r_f}=q''=\frac{q'''r_f}{2} \tag{4-29}$$

So,

$$C_1=-\frac{q'''r_f^2}{2} \tag{4-30}$$

$$k_c r\left.\frac{dT}{dr}\right|_{f}=-\frac{q'''r_f}{2} \tag{4-31}$$

We assume that k_c = constant,

$$\int_{T_g}^{T_c} dT=\int_{r_g}^{r_c}\frac{dr}{r}\frac{q'''r_f^2}{2k_c} \tag{4-32}$$

$$\Delta T\big|_{Clad}=-\frac{q'''r_f^2}{2k_c}\ln\left(\frac{r_c}{r_g}\right) \tag{4-33}$$

$$r_c=r_f+t_g+t_c \tag{4-34}$$

Since t_g is very small then by ignoring it one gets,

$$r_c=r_f+t_c \quad , r_g=r_f$$

$$\Delta T\big|_{Clad}=-\frac{q'''r_f^2}{2k_c}\ln\left(\frac{r_f+t_c}{r_f}\right) \tag{4-35}$$

With expanding the log we get,

$$r_f\ln\frac{r_f+t_c}{r_f}=r_f\ln(r_f+t_c)-r_f\ln r_f\approx t_c$$

$$\Delta T\big|_{Clad}=-\frac{q'''r_f}{2}\frac{t_c}{k_c}=\frac{q'}{2\pi r_f}\left(\frac{t_c}{k_c}\right) \tag{4-36}$$

See Appendix A for all the notations.

4.1.4. Heat Transfer from Cladding Surface to Coolant

Newton's law of cooling describes heat transfer from the clad surface to the coolant,

$$q'' = h_{wall}\left(T_c - T_b\right) \tag{4-37}$$

$$T_c - T_b = \frac{q''}{h_{wall}} \tag{4-38}$$

$$q'' = \frac{q''' r_f^2}{2r_c} \tag{4-39}$$

And, because $q' = \pi \cdot r_f^2 \cdot q''$, then

$$\Delta T\big|_{Cool} = T_c - T_b = \frac{q'}{2\pi r_c h_{wall}} \tag{4-40}$$

Where $r_c = r_f + t_c$

By taking the summation of all these separate temperature drops from the fuel centreline, which has the maximum temperature, to the coolant, one can get,

$$T_0 - T_b = \Delta T\big|_{Fuel} + \Delta T\big|_{Gap} + \Delta T\big|_{Clad} + \Delta T\big|_{Cool} \tag{4-41}$$

5. Numerical Solution of the Heat Conduction Problem

5.1. Transient Heat Conduction

During the course of its in-core life, a nuclear reactor fuel element normally experiences many thermal transients. These operational transients are associated with such things as reactor start up or shut down and changes in power level. In the case of very severe transients, the foregoing analytical techniques may not provide the desired accuracy due to large change in fuel temperature and coolant conditions. This fact with the obvious complexity of the analytical procedure and the availability of digital computers, has led to an increased use of numerical techniques. Discrete time and space intervals are considered and the general partial differential conduction equation (4-1) is rewritten in finite difference form. In the interest of simplicity, we neglect axial effects. To solve the transient temperature distribution equation (4.1) it must be finite differenced and numerically evaluated, according to the boundary conditions, which we described in Chapter 4.

$$\frac{1}{r}\frac{\partial}{\partial r}\left(kr\frac{\partial T}{\partial r}\right)+q'''=\rho Cp\frac{\partial T}{\partial t} \tag{5-1}$$

Three cases must be considered:

- Node on the centreline of the UO2 fuel pellet
- Interior nodes
- Boundary nodes

5.1.1. The node on the centreline of the UO2 fuel pellet

On the centreline, $r = 0$, the spatial derivative in Eq. (5.1) is undefined. By expanding the spatial derivative as,

$$\frac{1}{r}\frac{\partial}{\partial r}\left(kr\frac{\partial T}{\partial r}\right) = \frac{k}{r}\frac{\partial T}{\partial r}+\frac{\partial}{\partial r}\left(k\frac{\partial T}{\partial r}\right) \tag{5-2}$$

$$= \frac{k}{r}\frac{\partial T}{\partial r}+k\frac{\partial^2 T}{\partial r^2}+\frac{dk}{dT}\frac{\partial T}{\partial r}\frac{\partial T}{\partial r}$$

$$= \frac{k}{r}\frac{\partial T}{\partial r}+k\frac{\partial^2 T}{\partial r^2}+\frac{dk}{dT}\left(\frac{\partial T}{\partial r}\right)^2 \tag{5-3}$$

The symmetry condition, $\left.\frac{\partial T}{\partial r}\right|_{r=0}=0$, on the centreline implies that the last term on the right side of equation(5-3) vanishes and by using L'Hopital's rule,

$$\lim_{r\to 0}\frac{k}{r}\frac{\partial T}{\partial r}=k\left.\frac{\partial^2 T}{\partial r^2}\right|_{r=0} \tag{5-4}$$

$$\left.\frac{1}{r}\frac{\partial}{\partial r}(kr\frac{\partial T}{\partial r})\right|_{r=0}=2k\left.\frac{\partial^2 T}{\partial r^2}\right|_{r=0} \tag{5-5}$$

and the difference form of this equation is,

$$\left.\frac{1}{r}\frac{\partial}{\partial r}(kr\frac{\partial T}{\partial r})\right|_{r=0}=2k_1\frac{T_2-2T_1+T_o}{h^2}+O\left(h^2\right) \tag{5-6}$$

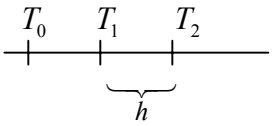

due to symmetry $T_o=T_2$ then,

$$\left.\frac{1}{r}\frac{\partial}{\partial r}(kr\frac{\partial T}{\partial r})\right|_{r=0}=4k_1\frac{T_2-T_1}{h^2} \tag{5-7}$$

$$=-\frac{4k_1}{h^2}T_1+\frac{4k_1}{h^2}T_2 \tag{5-8}$$

5.1.2. Interior Nodes

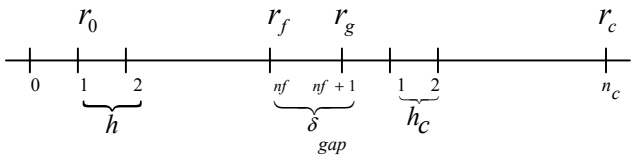

$$r_g-r_f=\delta_{gap}$$

$$r_c-r_g=\delta_{clad}$$

$$\left.rk\frac{\partial T}{\partial r}\right|_{r_{i+1/2}}=r_{i+1/2}k_{i+1/2}\left(\frac{T_{i+1}-T_i}{r_{i+1}-r_i}\right)+O\left(h^2\right) \tag{5-9}$$

$$\left.rk\frac{\partial T}{\partial r}\right|_{r_{i-1/2}}=r_{i-1/2}k_{i-1/2}\left(\frac{T_i-T_{i-1}}{r_i-r_{i-1}}\right)+O\left(h^2\right) \tag{5-10}$$

$$\left.\frac{1}{r}\frac{\partial}{\partial r}(kr\frac{\partial T}{\partial r})\right|_{r_i}=\frac{1}{r_i}\frac{1}{r_{i+1/2}-r_{i-1/2}}\left[\left(rk\frac{\partial T}{\partial r}\right)_{r_{i+1/2}}-\left(rk\frac{\partial T}{\partial r}\right)_{r_{i-1/2}}\right]+O\left(h^2\right) \tag{5-11}$$

The interior nodes in the fuel pellet, $i=2:n_f-1$

When h , h_c is constant step sizes in fuel pellet and cladding respectively, then by inserting Eq (5-9), (5-10) into Eq (5-11), we get,

$$\frac{1}{r}\frac{\partial}{\partial r}(k_f r\frac{\partial T}{\partial r})\bigg|_i = \frac{1}{r_i}\frac{1}{h^2}\left[k_{f(T_{i+1/2})}r_{(i+1/2)}(T_{i+1}-T_i)-k_{f(T_{i-1/2})}r_{(i-1/2)}(T_i-T_{i-1})\right] \qquad (5\text{-}12)$$

The interior nodes in the Zircaloy cladding, $i = n_f+1 : N-1$

$$\frac{1}{r}\frac{\partial}{\partial r}(k_c r\frac{\partial T}{\partial r})\bigg|_i = \frac{1}{r_i}\frac{1}{h_c^{\,2}}\left[kc_{(T_{i+1/2})}r_{(i+1/2)}(T_{i+1}-T_i)-kc_{(T_{i+1/2})}r_{(i-1/2)}(T_i-T_{i-1})\right] \qquad (5\text{-}13)$$

For all the notations we refer to Appendix A.

5.1.3. Boundary Nodes

First we consider the node at the surface of the fuel pellet:

$$\frac{1}{r}\frac{\partial}{\partial r}(kr\frac{\partial T}{\partial r})\bigg|_{r_{n_f}} = \frac{1}{r_{n_f}}\frac{1}{r_{n_f+1/2}-r_{n_f-1/2}}\left[\left(rk\frac{\partial T}{\partial r}\right)_{r_{n_f+1/2}}-\left(rk\frac{\partial T}{\partial r}\right)_{r_{n_f-1/2}}\right]$$

$$kr\frac{\partial T}{\partial r}\bigg|_{r_{n_f+1/2}} = h_{gap}\left(T_{n_f+1}-T_{n_f}\right)r_{(n_f+1/2)}$$

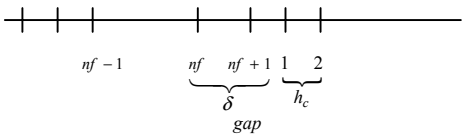

$$kr\frac{\partial T}{\partial r}\bigg|_{r_{nf-1/2}} = k_f(T_{n_f}-T_{nf-1})r_{(n_f-1/2)}\frac{T_{n_f}-T_{n_{f-1}}}{h}$$

$$\frac{1}{r}\frac{\partial}{\partial r}(k_f r\frac{\partial T}{\partial r})\bigg|_{r_{n_f}} = \frac{1}{h^*}\frac{1}{r_{n_f}}\left[h_{gap}r_{(n_f+1/2)}(T_{n+1}-T_n)-k_{f(T_{n_f-1/2})}r_{(n_f-1/2)}\frac{\left(T_{n_f}-T_{n_f-1}\right)}{h}\right] \qquad (5\text{-}14)$$

When $h^* = h+\dfrac{\delta_{gap}}{2}$ and $r_{(n_f+1/2)} = r_{n_f}+\dfrac{\delta_{gap}}{2}$

By the same way we can solve the nodes, at the inner surface and outer surface of the cladding,

The node at the inner surface of the cladding:

$$\frac{1}{r}\frac{\partial}{\partial r}(kr\frac{\partial T}{\partial r})\bigg|_{r_{n_f+1}} = \frac{1}{h^+}\frac{1}{r_{n_f+1}}\left[-h_{gap}r_{(nf+1-1/2)}\left(T_{nf+1}-T_{nf}\right)+kc_{(T_{nf+1+1/2})}r_{(n_f+1/2+1)}\left(T_{nf+2}-T_{nf+1}\right)\right] \qquad (5\text{-}15)$$

When $h^+ = h_c+\dfrac{\delta_{gap}}{2}$ and $r_{(n_f+1-1/2)} = r_{n_f}+\dfrac{\delta_{gap}}{2}$, $r_{(n_f+1+1/2)} = r_{n_f+1}+\dfrac{h_c}{2}$

Here δ_{gap} denotes gap thickness and δ_{clad} is cladding thickness.

The node at the outer surface of the cladding:

$$\frac{1}{r}\frac{\partial}{\partial r}(k_c r\frac{\partial T}{\partial r})\bigg|_{r=N} = \frac{1}{h_c}\frac{1}{r_N}\left[q_{wall}r_{(N+1/2)} - kc_{(T_{N-1/2})}r_{(N-1/2)}\frac{T_N - T_{N-1}}{h_c}\right] \tag{5-16}$$

$$q''_{wall} = h_{wall}(T_{N+1} - T_N) \tag{5-17}$$

Where, $T_{N+1} = T_b$

$$r_{i+1/2} = \frac{r_{i+1} + r_i}{2}$$

$$k_{i+1/2} = k\left(\frac{T_{i+1} + T_i}{2}\right), \qquad i = 1,2....., N-1, N$$

$$r_i = r_{i-1} + h, \qquad i = 1,2.....n_f, r_0 = 0$$

$$r_{c_i} = r_f + \delta_{gap} + ih_c, \qquad i = 1,2.....n_c$$

$$h = \frac{r_f}{n_f}, h_c = \frac{\delta_{clad}}{n_c}$$

For the notations refer to Appendix A and B.

5.2. Numerical Solution

Two classes of methods, explicit and implicit, that might be used in numerical solution are discussed below. It is well known that the explicit method is easy to set up and program. However, it has limited stability properties, which limit the size of the time step Δt, relative to the spatial step h, hence long computer running times.

Let us use an explicit method in our numerical solution on the heat conduction equation (5-1)

$$\rho Cp\frac{\partial T}{\partial t}=\frac{1}{r}\frac{\partial}{\partial r}\left(rk\frac{\partial T}{\partial r}\right)+q'''$$

In the explicit method we replace time and space derivatives with the following approximations:

$$\frac{\partial T}{\partial t}\Big|_i=\frac{T_i^{j+1}-T_i^{j}}{\Delta t}+O(\Delta t) \qquad (5\text{-}18)$$

$$\frac{\partial^2 T}{\partial r^2}=\frac{T_{i+1}{}^{j}-2T_i^{j}+T_{i-1}{}^{j}}{h^2}+O\left(h^2\right) \qquad (5\text{-}19)$$

By inserting these finite difference forms (5-18) and (5-19) into the general transient conduction equation one can get,

$$\overline{T}^{j+1}=\overline{T}^{j}+\Delta t\,A^j\overline{T}^{j}+b^j \qquad (5\text{-}20)$$

Where:

A^j is a matrix, its coefficients is shown in Table-1, and b^j is the right hand side of the matrix, which contains a vector of volumetric heat source q''' with the boundary conditions.

$$b=\frac{1}{\rho c_p}\left[q_1{}''',q_2{}''',\cdots\cdots q_N{}'''+\frac{h_{wall}r_{N+1/2}}{h\,r_N}\right] \qquad (5\text{-}21)$$

As it is described above we are using a forward difference in equation (5-18), but a central difference in equation (5-19). The stability condition for the explicit method is:

$$\frac{k\Delta t}{\rho c_p h^2}\le\frac{1}{2},\ \Delta t\le\frac{\rho c_p h^2}{2k}$$

5.2.1. Implicit Method

An implicit method has better stability , which translates into less computation time because a larger Δt may be taken.

$$\rho Cp\frac{\partial T}{\partial t}=\frac{1}{r}\frac{\partial}{\partial r}\left(rk\frac{\partial T}{\partial r}\right)+q'''$$

With the implicit method we get,

$$\overline{T}^{j+1}=\overline{T}^{j}+\Delta t\left(A^{j+1}\overline{T}^{j+1}+b^{j+1}\right) \tag{5-22}$$

$$\overline{T}^{j+1}-\Delta tA^{j+1}\overline{T}^{j+1}=\overline{T}^{j}+\Delta t\,b^{j+1} \tag{5-23}$$

$$\underbrace{\left(I-\Delta tA^{j+1}\right)}_{C}\overline{T}^{j+1}=\underbrace{\overline{T}^{j}+\Delta t\,b^{j+1}}_{W} \tag{5-24}$$

$$\overline{T}^{j+1}=C^{-1}W \tag{5-25}$$

There is no stability problem; any Δt will give a stable solution. Only accuracy requirements are needed to think about when Δt is chosen.

A and b are the same as they are described in explicit method.

5.2.2. Crank-Nicolson Method

Crank and Nicolson have suggested an implicit method that essentially eliminates the stability problem experienced in explicit schemes. The basis for this method is to substitute the arithmetic average of the temperature at the present and future time step into the spatial derivatives. That means that $T_i^{\,j}$ would be replaced by $\left(T_i^{\,j}+T_i^{\,j+1}\right)/2$.

The resultant spatial derivatives can be combined with the temporal derivative, given by equation (5-18),

$$\rho c_p\frac{\partial T}{\partial t}=\frac{1}{r}\frac{\partial}{\partial r}\left(kr\frac{\partial T}{\partial r}\right)$$

$$\frac{\partial^2 T}{\partial r^2}\approx\frac{1}{2}\left[\frac{T_{i+1}{}^{j}-2T_i^{\,j}+T_{i-1}{}^{j}}{h^2}+\frac{T_{i+1}{}^{j+1}-2T_i^{\,j+1}+T_{i-1}{}^{j+1}}{h^2}\right] \tag{5-26}$$

$$\overline{T}^{j+1}=\overline{T}^{j}+\frac{\Delta t}{2}\left(A^{j+1}\overline{T}^{(j+1)}+b^{j+1}+A^{j}\overline{T}^{j}+b^{j}\right) \tag{5-27}$$

In a modified version of Crank-Nicolson we use A^j instead of A^{j+1}

$$\underbrace{\left(I-\frac{\Delta t}{2}A^{j}\right)}_{C^{j}}\overline{T}^{\,j+1}=\underbrace{\overline{T}^{\,j}+\frac{\Delta t}{2}\left(A^{j}\overline{T}^{\,j}+b^{j}+b^{j+1}\right)}_{W^{j}} \tag{5-28}$$

$$\overline{T}^{\,j+1}=\left(C^{j}\right)^{-1}w^{j} \tag{5-29}$$

$\overline{T}^{\,j}$: is a temperature vector at time t ,

$$\overline{T}^{\,j}=\left(T_1{}^{j},T_2{}^{j},\ldots T_N{}^{j}\right)^{T}, \tag{5-30}$$

$\overline{T}^{\,j+1}$: is a temperature vector at time $t+\Delta t$

$$\overline{T}^{\,j+1}=\left(T_1{}^{j+1},T_2{}^{j+1},\ldots T_N{}^{j+1}\right)^{T}, \tag{5-31}$$

We define $q=q'''$ then,

$$b^{j}=\frac{1}{\rho c_p}\left[q_1{}^{j},q_2{}^{j},\cdots\cdots q_N{}^{j}+\frac{h_{wall}r_{N+1/2}}{hr_N}\right] \tag{5-32}$$

$$b^{j+1}=\frac{1}{\rho c_p}\left[q_1{}^{j+1},q_2{}^{j+1},\cdots\cdots q_N{}^{j+1}+\frac{h_{wall}r_{N+1/2}}{hr_N}\right] \tag{5-33}$$

A^{j} is a tridiagonal matrix, the coefficients of the matrix is shown in Table -1

$$A^{j}=\frac{1}{h^{2}}\begin{bmatrix} b_1 & c_1 & & & & & & & \\ a_2 & b_2 & c_2 & & & & & & \\ & a_3 & b_3 & c_3 & & & & & \\ & & a_i & b_i & c_i & & & & \\ & & & \ddots & \ddots & \ddots & & & \\ & & & & a_{n_f} & b_{n_f} & c_{n_f} & & \\ & & & & & a_{n_f+1} & b_{n_f+1} & c_{n_f+1} & \\ & & & & & & \ddots & \ddots & \\ & & & & & & & a_N & b_N \end{bmatrix}$$

where:

h	constant grid step sizes
Δt	time step sizes

h from the centre of the fuel (r=0, i=1) to the fuel surface ($r=r_f$, $i=n_f$) is equal to fuel pellet step size (h) and from cladding inner surface ($r=r_g$, $i=n_{f+1}$) to the outer cladding surface ($r=r_c$, $i=N$) is cladding step size(h_c)and δ_{gap} is the gap width between fuel and cladding.

In the Crank-Nicolson method, we interpret the finite-difference approximation to the time derivative as a central difference at the midpoint of the time interval. The most important advantage of this method is that it is stable.

That means there is no instability problem. The Crank-Nicolson method is a technique that makes its finite difference approximation of the same order for the spatial and the time derivatives .

Temperature distribution has been plotted by using equations in chapter (3) for thermo-physical properties in fuel, gap and cladding, the initial and boundary conditions used are:

$q''' = 30MW$, $T_b = 280C$, $R_{ca} = 6.125.10^{-3} m$, $drca = 80.10^{-4} m$,

$\delta_{gap} = 0.105.10^{-3} m$, $tol = 0.001$, $h_{wall} = 25.10^4 \ W.m^{-1}.K^{-1}$, $h_{gap} = 10^4 \ W.m^{-1}.K^{-1}$

For all the notations we refer to Appendix A and B.

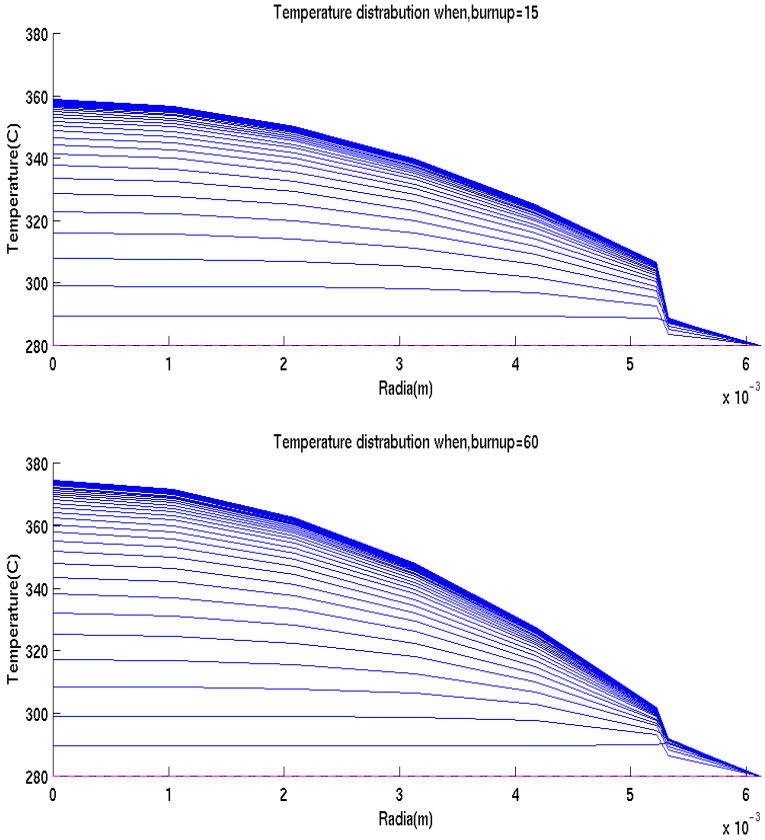

Figure 5-1:Transient Temperature Distribution Using Crank Nicolson method.

5.2.3. MATLAB COMMAND (ODE15S)

`ODE15S` is a MATLAB time integrator for initial-value problems, especially suited for discretized parabolic PDE's such as the heat equation of Ch. 4. ODE15S uses Backward Differentiation formulas – the "Gear Method" – in a variable stepsize, variable order scheme.

`[T, U] = ODE15S (ODEFUN, TSPAN, U0)` with `TSPAN = [T0 Tend]`

Integrates the ODE $u' = f(t, u)$ from initial time (*t0*) to final time (*tend*) with initial conditions (*u0*).

The plot below shows the steady state temperature distribution in the fuel element, obtained by taking *Tend* large, and using the same initial and boundary conditions as it is given in Crank Nicolson plot.

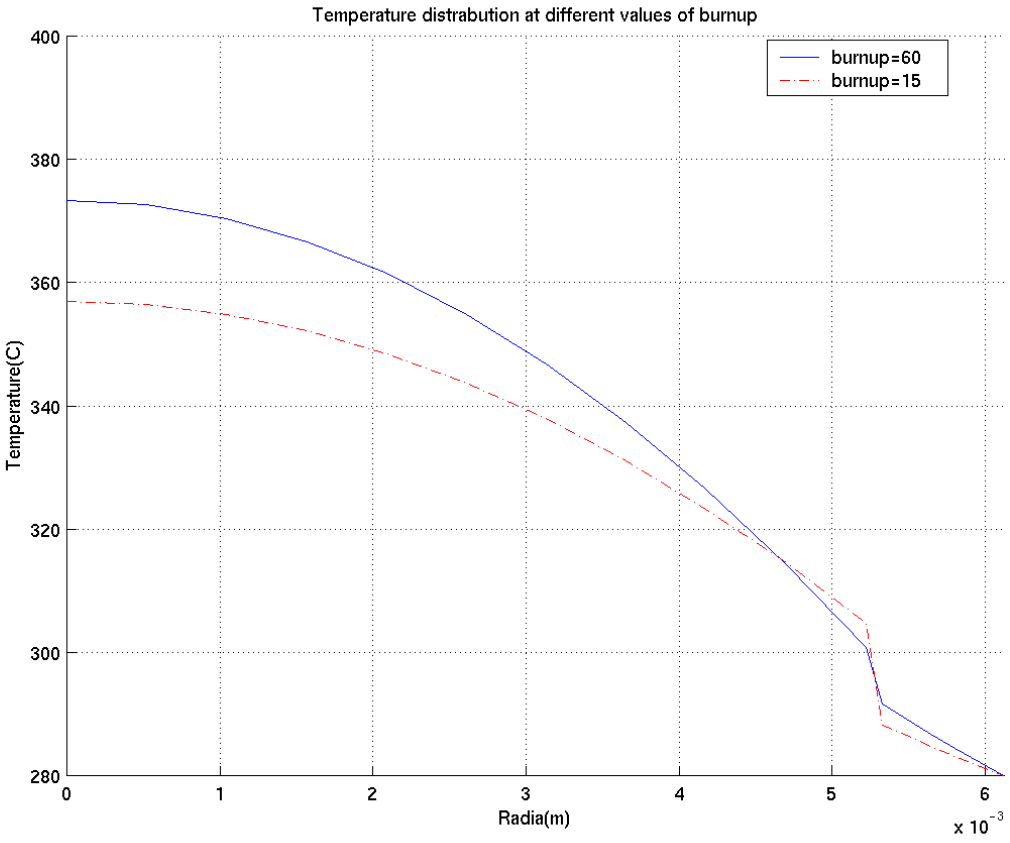

Figure 5.2: Temperature Distribution Using MATLAB Command (ODE15S)

5.3. Steady-State Heat Conduction

A very similar analysis can be performed on the steady–state version of equation (5-1) to yield the finite difference formulation of the steady state conduction. To start the calculation, we will use the iterative method to get the initial temperature distribution for given internal generation vector q'''.

$$\Rightarrow \frac{1}{h^2}\begin{bmatrix} b_1 & c_1 & & & & & & & \\ a_2 & b_2 & c_2 & & & & & & \\ & a_3 & b_3 & c_3 & & & & & \\ & & a_i & b_i & c_i & & & & \\ & & & \ddots & \ddots & \ddots & & & \\ & & & & a_{n_f} & b_{n_f} & c_{n_f} & & \\ & & & & & a_{n_f+1} & b_{n_f+1} & c_{n_f+1} & \\ & & & & & & \ddots & \ddots & \\ & & & & & & & a_N & b_N \end{bmatrix} \begin{bmatrix} T_1 \\ T_2 \\ \vdots \\ \vdots \\ \vdots \\ T_{nf} \\ T_{nf+1} \\ \vdots \\ \vdots \\ T_N \end{bmatrix} + \frac{1}{\rho c_p}\begin{bmatrix} q''' \\ \vdots \\ \vdots \\ \vdots \\ \vdots \\ 0 \\ \vdots \\ \vdots \\ \dfrac{h_{wall}\left(r_{N+1/2}\right)}{h\, r_N} \end{bmatrix} = 0$$

Where T is the vector of temperature values**,** A, h and b are the same as they are described in section (5.2.3.).

The thermal properties of specific heat and thermal conductivity make the system non linear. The non linearity of the system depends on the material and the range of the temperature variation .We will use Newton's method to solve the system.

5.3.1. Newton Iteration Process

One of the most widely used methods of solving non-linear equations is Newton's method; this method is based on a linear approximation of the function. Starting from an initial estimate, we calculate the next approximation. This is continued until an estimate of the error due to terminating the iteration is less than a user specified tolerance. We will use the norm as a measure of how close **f(u)** is to zero. By insisting that the norm of **f(u)** should be smaller than some small tolerance, we ensure that all the elements in **f(u)** are numerically smaller than the tolerance.

In order to update the estimate, Newton's method linearises the function around the last estimate, i.e. if u_k is the last estimate we get

$$f(u_k) \approx f(u_k) + J(u_k)(u - u_k) = P(u) \qquad (5\text{-}34)$$

Then we choose the new estimate, $u_{k+1,}$ so that $P(u_{k+1}) = 0,$ i.e.

$f(u_k) + J(u_k)(u_{k+1} - u_k) = 0$

When introducing $\delta = u_{k+1} - u_k$ we get $J(u_k)\delta = -f(u_k)$

This is obviously a linear equation with

$$\delta = -J^{-1} f$$

Where the jacobian matrix is evaluated at u_k and the next Newton iterate is obtained by $u_{k+1} = u_k + \delta$. (5-35)

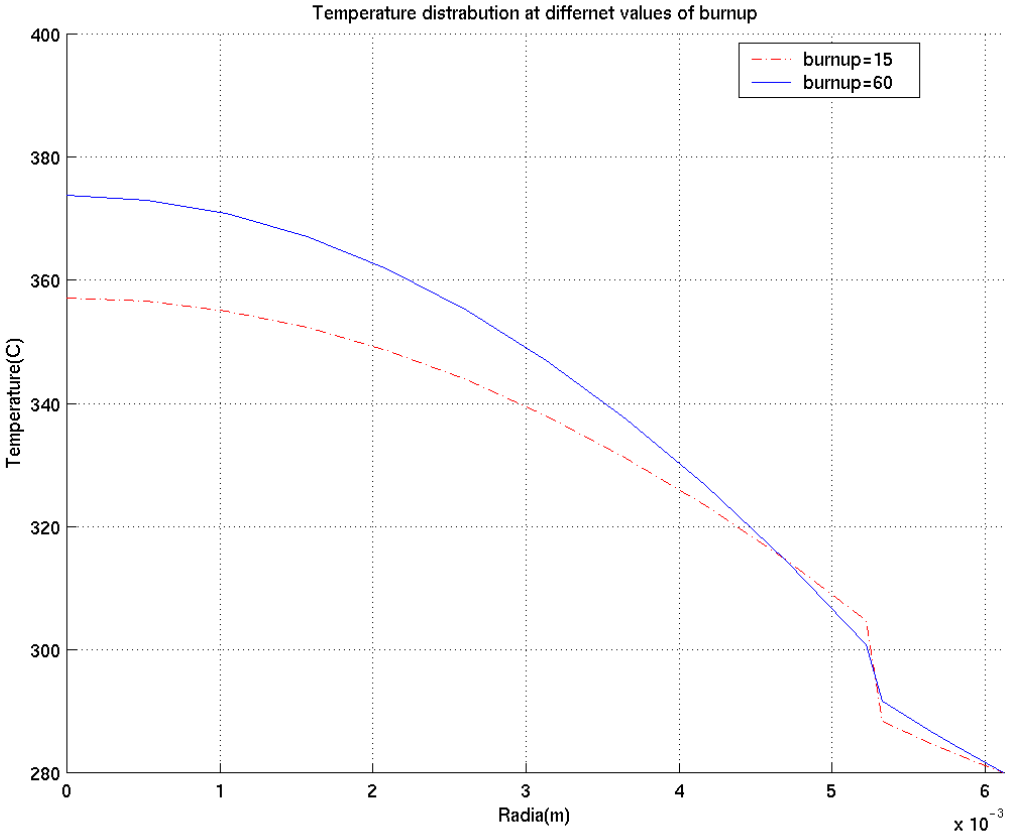

Figure 5.3: Steady Temperature Distribution Using Newton's Method.

Starting with T_b (bulk or fluid temperature) as an initial guess and taking that as the next approximation, this is continued until the error is less than tolerance (*tol*) [Appendix B], which specifies by user as an input.

5.3.2. Jacobian Matrix by Numerical Differentiation

In Newton's method, it is necessary to know the jacobian matrix of the vector equation .The jacobian is frequently computed approximately by numerical differentiation. We make a small perturbation to one of the **u** elements (keeping the other constant), evaluate the function and use the difference in function value over the perturbation as a measure of the differential with respect to this **u** element. If **s** is the size of the **j**-th perturbation and $\mathbf{e_j}$ is the unit vector with one in the **j**-th element and zero else then the jacobian elements in the point **u** are calculated as:

$$J_{i,j} \approx D_{i,j} = \frac{f_i\left(u + s_j e_j\right) - f_i(u)}{s_j} \qquad ,i,j = 1,....n \qquad (5\text{-}36)$$

The size of perturbation **s** is very important for the accuracy of the approximation. The choice of perturbation is a trade off between making the perturbation as small as possible to improve the theoretical accuracy while at the same time not making it so small that the round-off accuracy of the computer becomes limiting.

Note that when *J* is sparse, it is sometimes possible to compute it by fewer than *N* evaluations of *f*, by perturbing several elements of *u* at once.

For example, in the case at hand *J* is tri-diagonal and four evaluations suffice.

6. Conclusions

In this master thesis we have implemented a steady state and transient thermal radial heat conduction model for the fuel elements. Since, analytical solution of this model is rather involved, and it is application to the actual heat calculation in a fuel element is not so frequent, for many reasons, like temperature dependence properties, it is preferred to perform the calculation of the heat conduction by numerical methods. In this report:

- We have defined a new nodalization for fuel pellet, gap and cladding by taking an arbitrary number of cylindrical regions and using constant step sizes for fuel and cladding, and a small gap thickness between them is considered.
- Advanced thermo physical properties for each material have been investigated and computed by using a temperature dependence expression for each property.
- We have included the effect of burnup on the thermal conductivity of fuel pellets while its effects are ignored in RAMONA [1].
- We have presented numerical methods, Explicit method, Implicit method, Crank-Nicolson, and the standard MATLAB integrator ODE15S with their stability conditions, showing that there is no stability problem in Crank Nicolson method.
- The last part of the job was implementation of the MATLAB program in MATSTAB, for analysing and computing steady state temperature distribution in fuel, gap and cladding including investigated temperature-dependent material properties.
- The performance was evaluated on a test case; Profiling of the code indicates that simple optimisations will cut the runtimes by at least a factor of five.

Performance timing:

The test case was on 8450 radial elements and 10 nodes per each element, the run-time (CPU time) was about fifty minutes i.e. about 3000 sec. From the Matlab Profile Report Appendix C we found that:

1- The code calls the eq_DtfDt0 function 411048 times, where the function returns the finite differencing matrix, and the run-time is about 2381 seconds.

2- The code calls the fcoeffHgap function 411048 times, where the function is used for calculating the coefficients of the polynomial gap heat transfer approximation, and the run-time is 680 seconds.

The code can be optimized to run faster without changing the computed results if the optimisation process includes:

- Improving the Jacobian finite differencing.
- Reducing the number of nodes per each element, which reduces the run-time by a factor of about three.
- Reducing the number of the fcoeffHgap function calls transfer by calling ones instead of (411048), since the coefficients are the same for all the radial elements.

Acknowledgment

I would like to thank all the people at the department of numerical analysis and scientific computing at Royal Institute of Technology (NADA-KTH). I'm especially grateful to my supervisor Gerd Eriksson for sharing her time and knowledge with me. And I'm very grateful to Professor Jesper Oppelstrup for his advice and Dr. Lennart Edsberg the master program coordinator. I'm also grateful to Katarina Gustavsson at NADA for her support.

And I would like to thank all the people at Vattenfall Bränsle. I owe many thanks to my tutor Marek Kosinski for much good advice and to Dr. Jan Almberger for his support during these months.

Table –1

We define: $\ell_{f_i} = \frac{1}{\rho_i c_{p_i}}\Big|_{fuel}$, $\ell_{c_i} = \frac{1}{\rho_i c_{p_i}}\Big|_{clad}$

The elements of the tridiagonal matrix, A

$$b_1 = \ell_{f_1}(-4k_f(T_1))$$
$$c_1 = \ell_{f_1}(4k_f(T_1))$$

$$a_i = \frac{\ell_f}{ri}\left(k_f(T_{i-1/2})r_{(i-1/2)}\right)$$
$$b_i = \frac{\ell_{f_i}}{r_i}\left(k_f(T_{i+1/2})r_{(i+1/2)}\right)$$
$$c_i = \frac{\ell_{f_i}}{r_i}\left(\left(k_f(T_{i+1/2})r_{(i+1/2)}\right)+\left(k_f(T_{i-1/2})r_{(i-1/2)}\right)\right)$$

$$a_{n_f} = \frac{\ell_{f_i}}{r_{nf}}\left(k_f(T_{n-1/2})r_{(n-1/2)}\right)$$
$$b_{n_f} = \frac{\ell_{f_i}}{r_{nf}}\left(k_f(T_{n-1/2})r_{(n-1/2)} + r_{n+1/2}h_{gap}h\right)$$
$$c_{n_f} = \frac{\ell_{f_i}}{r_{nf}}\left(r_{n+1/2}h_{gap}h\right)$$

$$a_{nf+1} = \frac{\ell_{ci}}{r_{nf+1}}\left(h\,r_{(n+1/2)}h_{gap}\right)$$
$$b_{nf+1} = \frac{\ell_{c_i}}{r_{nf+1}}\left(-k_c\left(T_{n+1+1/2}\right)r_{(n+1+1/2)} - h\,r_{(n+1/2)}h_{gap}\right)$$
$$c_{nf+1} = \frac{\ell_{c_i}}{r_{nf+1}}\left(k_c\left(T_{n+1+1/2}\right)r_{(n+1+1/2)}\right)$$

$$a_N = \frac{\ell_{c_i}}{r_N}\left(h\,r_{(n+1/2)}h_{gap}\right)$$
$$b_N = \frac{\ell_{c_i}}{r_N}\left(-k_c\left(T_{N-1/2}\right)\left(r_{N-1/2}\right)+ h\,r_{(N+1/2)}h_{wall}\right)$$

Table-2

Gap Heat Transfer Coefficients as a Function of temperature and Burnup

Burnup	363°C	439°C	520°C	598°C	678°C
0.0 MWd/kgU	4700	5000	5400	5800	6400
0.5 *MWd/kgU*	4700	5000	5400	5900	6400
1.0 MWd/kgU	4800	5100	5400	5900	6500
2.0 *MWd/kgU*	4800	5100	5500	6000	6600
3.0 *MWd/kgU*	4900	5200	5600	6100	6700
5.0 *MWd/kgU*	5100	5400	5900	6400	7100
7.5 MWd/kgU	5200	5600	6100	6700	7500
10.0 *MWd/kgU*	5400	5800	6400	7000	7900
12.5 *MWd/kgU*	5600	6000	6600	7300	8300
15.0 *MWd/kgU*	5800	6300	6900	7700	8800
17.5 *MWd/kgU*	6000	6500	7200	8100	9400
20.0 *MWd/kgU*	6200	6800	7600	8600	10000
25.0 MWd/kgU	6800	7500	8400	9700	11700
30.0 *MWd/kgU*	7400	8200	9500	11200	13900
35.0 *MWd/kgU*	8200	9200	10800	13100	17300
40.0 *MWd/kgU*	9100	10500	12700	16100	23100
45.0 *MWd/kgU*	10400	12300	15600	21100	27800
50.0 *MWd/kgU*	12300	14900	20200	26400	30300

Appendix A

k_f =Fuel thermal conductivity ($W.m^{-1}.K^{-1}$)

k_g =Gap thermal conductivity ($W.m^{-1}.K^{-1}$)

k_c =Clad thermal conductivity ($W.m^{-1}.K^{-1}$)

h_{gap} =Gap heat transfer coefficient ($W.m^{-1}.K^{-1}$)

h_{wall} =Convective heat transfer coefficient ($W.m^{-1}.K^{-1}$)

r_f =Fuel pin surface radius (m)

$t_g = \delta_{gap}$ =Gap thickness (m)

t_c =Clad thickness (m)

T_o =Fuel centreline temperature (K)

T_f = Fuel surface temperature (K)

T_g =Inside surface temperature of the clad (K)

T_c =Outer clad surface temperature (K)

T_b =Bulk temperature (K)

q''' =Volumetric heat source (W)

q' =Linear power density $(W.m^{-1})$.

c_p =Specific heat ($J/k_g.K$)

ρ =Density (kg/m^3)

b =Burn up in atoms % ,1at.%=9.383 MWd/kgU

Appendix B

Input fuel parameters to the code:

R_f =Fuel pellet radius (m)

Rca =Total fuel radius (m)

$drca$ =Cladding thickness (m)

δ_{gap} =Gap thickness (m)

n_f =Number of fuel zones

n_c =Number of cladding zones

tol =Maximum tolerance (related to the local error bound that the user aims to achieve)

T_b =Fluid temperature(C)

b =Burn up in atoms%(1 atom%=9.383GWD/MTU at 200MeV/fisson).

q''' =Volumetric heat source (Watt)

Appendix C

MATLAB Profile Report: Summary

Report generated 12-Feb-2003 17:07:20

```
Total recorded time:      3149.40 s
Number of M-functions:          98
Number of M-subfunctions:        7
Number of M-scripts:             2
Number of MEX-functions:         2
Clock precision:             0.010 s
```

Function List

Name	Time		Calls	Time/call	Self time	
run_mstab	3149.080	100.0%	1	3149.080000000	0.040	0.0%
matstab	3149.040	100.0%	1	3149.040000000	0.350	0.0%
steady_state	3145.540	99.9%	1	3145.540000000	0.030	0.0%
power_void	3145.510	99.9%	1	3145.510000000	0.090	0.0%
eq_tftc	3144.490	99.8%	1	3144.490000000	221.830	7.0%
eq_DtfDt0	2381.070	75.6%	411048	0.005792681	1452.610	46.1%
fcoeffHgap	679.820	21.6%	411048	0.001653870	679.820	21.6%
eq_Qf0	541.500	17.2%	411048	0.001317364	373.870	11.9%
eq_denf	72.790	2.3%	822096	0.000088542	72.790	2.3%
eq_kf	72.660	2.3%	822096	0.000088384	72.660	2.3%
eq_capf	68.900	2.2%	822096	0.000083810	68.900	2.2%
eq_kc	68.470	2.2%	822096	0.000083287	68.470	2.2%
eq_capc	66.910	2.1%	822096	0.000081390	66.910	2.1%
eq_denc	66.540	2.1%	822096	0.000080939	66.540	2.1%
get_inp	2.890	0.1%	1	2.890000000	0.280	0.0%

References

[1] W.Wulff, H.S.cheng, D.S.Diamond, and M.khatib-Rahbar ’’ A Description and Assessment of RAMONA-3B Mod. O cycle 4:A Computer Code with Three-Dimensional neutron kinetics for BWR System Transients.

[2] Philipp Hänggi’’Investigation BWR Stability with a New Linear Frequency-Domain Method and Detailed 3D.Neutronics’’.

[3] R.T.Lahey, Jr.&F.J.Moody‘’The Thermal Hydraulics Of A Boiling Water Nuclear Reactor’’.

[4] Neil E. Todreas, Majid S. Kazimi Taylor and Franci, 2001,” Nuclear System Elements of thermal hydraulic design”.

[5] Curtis F. Gerald, Patrick O. Wheatly “Applied Numerical Analysis ” sixth addition.

[6] D.D.Lanning.C.E.Buyer and C.L.Painter ’’FRAPCON-3: Modification to Fuel Rod Materials Properties and Performance Modes for High-Burnup Applications’’ October 1997.

[7] James J.Duderstadt, Louis J.Hamilton ‘’ Nuclear Reactor Analysis’’.

[8] http://www.insc.anl.gov.

[9] A test on gap heat transfer as a function of temperature and burn up.